MALMBERG, D., BJÖRKVALL, J., MALM, J. and BÅÅTH, L. Preliminary microwave measurements on liquid slags. *VII International Conference on Molten Slags Fluxes and Salts,* The South African Institute of Mining and Metallurgy, 2004.

Preliminary microwave measurements on liquid slags

D. MALMBERG*, J. BJÖRKVALL*, J. MALM† and L. BÅÅTH†

**MEFOS, Luleå, Sweden, †University of Halmstad, Halmstad, Sweden*

Microwave technology has for decades been a tool for astronomers to map and understand the complexities of the universe its composition and extent. It is also used on a laboratory scale by spectroscopists to examine properties of atomic and molecular compounds. In this novel work we will introduce microwave technology to be used for the investigation of liquid slag structures. The preliminary results indicate that the alteration of the slag composition could be correlated to the measured microwave refractive index. Investigations have been performed in the Al_2O_3-CaO-SiO_2 slag system.

Keywords: Microwave technology, slag, structure, liquid, Al_2O_3-CaO-SiO_2

Introduction

Electromagnetic waves may penetrate media of varying physical properties, resulting in a change of their amplitude, phase and polarization, a change representative of the media being penetrated. In this respect, changes in the pattern and polarization of electromagnetic wave fronts represent the most sensitive probes in physics. Radio astronomical techniques, and especially interferometer techniques where one has direct access to the wave front data, are very well suited to be used for any such probes. In Figure 1 is an image of a molecular cloud in the universe derived with such a technique.

Turning the focus towards closer objects and using a similar technological approach, it would be possible to investigate slag properties, solid and liquid, by exposing the slag to electromagnetic radiation of suitable frequencies where the changes in the wave pattern, representing slag properties, are measured and exploited in order to comprehend slag properties.

If a microwave signal is transmitted towards and reflected at a surface (slag or metal), then the phase of the signal will change linearly with frequency since a delay between the reference and object signals, offset from zero in the time plane, will correspond to a phase slope in the frequency plane. If the signal is instead transmitted towards a semitransparent medium, then part of the signal will be reflected. Part of it will also be refracted and propagate through the medium to be reflected at the next surface where the index of refraction again changes. These double, or multiple, reflected waves will, when cross-correlated with the reference signal, show a more complicated curve of phase as a function of frequency. If data therefore are sampled as complex cross-correlated amplitudes in frequency channels over a frequency band, then the distances to both or all the surfaces can be recovered.

If then, as in the astrophysical case, the signal is transmitted and received by an interferometer in the aperture plane, the full three-dimensional structure of the volume can be reconstructed. If the data are sampled from a single point only, then only the depth (thickness) information can be reconstructed. It is this latter approach that is being used in this presentation. Both solid and liquid slag has been investigated but in the context of this paper only the liquid slag will be reported.

Objectives

The long-term objective is to use microwave technology to quantify the slag metallurgical performance in a specific process step during steel production. This work includes the evaluation of the dielectric properties of the slag and thus the refractive index for the slag.

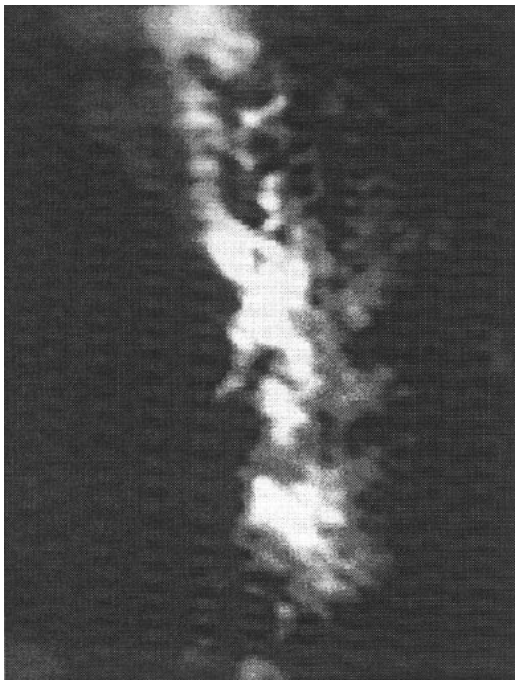

Figure 1. Molecular Cloud (Orion Nebula)

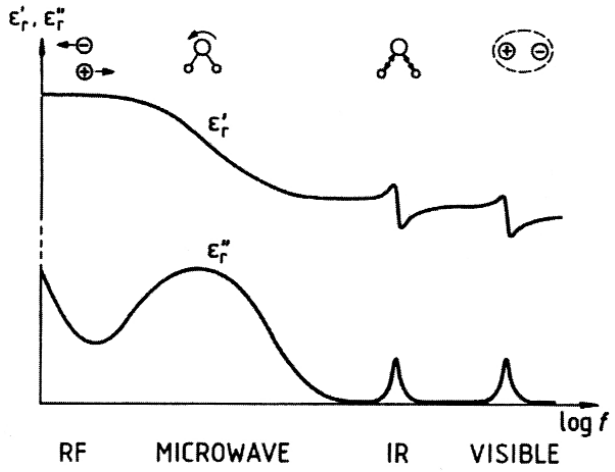

Figure 2. Parameters affecting the dielectric constant [1]

Technology

The focus in the series of trials has been on establishing the dielectric properties of the slag and, by extension, also the refractive index. In Figure 21 it can be seen which physical mechanism contributes to the magnitude of the constant and also that the constant is a complex number. However, in the investigation the measured value of the index has not been separated into its real and imaginary parts.

Antenna radiation pattern

Optics in the microwave range of the electromagnetic spectrum is usually called antenna and its resolution is restricted by the antenna diameter, i.e. diffraction. When using an antenna for measurements in a metallurgical process, it is important to find out in which way its radiation pattern coincides with the surrounding environment e.g. the furnace opening. Once this has been decided the measurements can proceed without interference.

The radiation from the antenna varies with distance. The space surrounding it could be divided into three different regions, each one with its own typical impact on antenna sensitivity and signal interference. The field regions are illustrated in Figure 3.

- Reactive near-field
- Radiating near-field (Fresnel region)
- Far-field (Fraunhofer region)

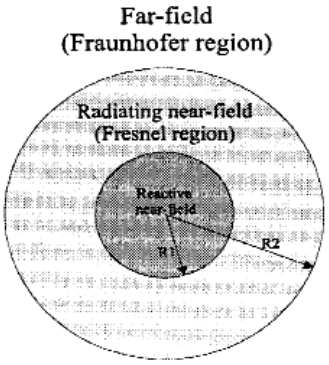

Figure 3. Field regions

The reactive near-field region exists at a distance $R < 0{,}62(D^3/\lambda)^{1/2}$ from the antenna opening where λ is the wavelength, R is the range and D is the antenna aperture. Within this distance the reactive near-field dominates the signal. Normally this field is of no significance for our measurements, with one exception. If the antenna must be protected from heat radiation from the furnace a ceramic disk, a piece of refractory, will be positioned directly in front of the antenna but at a distance determined by the equation for the reactive near-field.

The radiating near-field is defined as the field of the antenna between the reactive near-field region and the far-field region. This field is restricted to an inner boundary defined by $R \geq 0{,}62(D^3/\lambda)^{1/2}$ and the outer boundary defined by $R < 2D^2/\lambda$ and is of no significance for our measurements whatsoever.

The far-field region is defined as 'that region of the field where the angular field distribution is essentially independent of the distance from the antenna' and can be written as $R > 2D^2/\lambda$. It is in this region the measurements takes place.

A deeper analysis of antenna properties can be found in Electromagnetic Horn Antennas[2] and Antenna Theory[3].

Signal performance

A microwave signal at a well-defined frequency is transmitted from the antenna towards the surfaces of the slag and metal bath. The reflected signal is received in the same antenna and the difference in phase between the transmitted and received signal is recorded. The difference in phase is a direct measure of that fraction of a wavelength

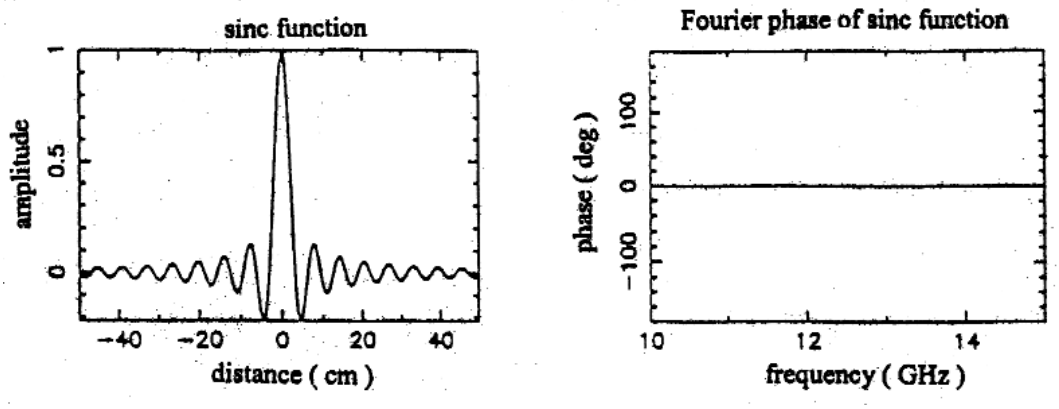

Figure 4a. Changes in phase difference

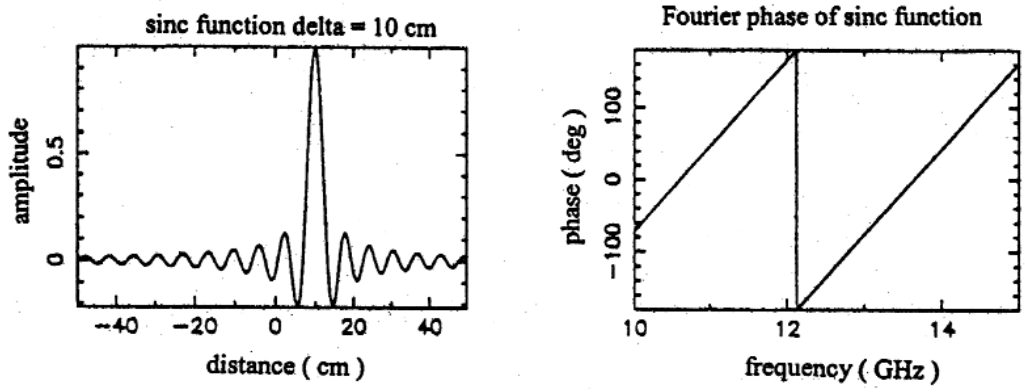

Figure 4b. Changes in phase difference

the reflected wave has travelled compared with the signal transmitted what is left to solve is the number of full wavelengths that must be added to the fraction in order to find the full distance.

Stepping in phase within a frequency band with a bandwidth, $\omega_h - \omega_l = \Delta\omega$, and then measuring the phase difference for each frequency step, solves this. This procedure is repeated over a number of frequency steps, in this case frequency channels within the frequency band, Σm, each with an individual bandwidth of $\Delta\omega/\Sigma m$ depending on the maximum distance to be measured and the required resolution. The difference in phase between transmitted and received signal is thereafter recorded for each channel and where each channel gives the distance to the reflecting surface as an unspecified number of wavelengths plus a known part of the wavelength. By measuring the phase difference over a great number of frequency channels, the distance can be measured as the curvature of phase difference versus frequency and then Fourier transformed from the frequency domain to the time domain. The change in phase difference with frequency is a straight line whose derivative is a direct measure of the extra distance the reflected wave has travelled, as seen in Figure 4a.

When the signal is transmitted towards a surface of slag on top of metal, two waves will be reflected, one from the slag surface, the other from the metal. The reflected waves will be added, resulting in a typical pattern that is recorded, and its phase is compared with the transmitted wave. The resulting phase difference with frequency is no longer an inclined straight line but a more complicated curve, as shown in Figure 4b.

The shape of the curve depends on the position of the reflecting surface's positions related on the reference position of the transmitted wave. In this way the slag thickness and refractive index can be evaluated.

Experimental procedure

Each liquid slag was investigated by sweeping it in different frequency band of 4 GHz bandwidth, where each frequency band consists of 501 frequency channels. The investigation has focused on a few dominant slag constituents rather than on a complete slag. The measurement instrumentation used during the trials is enumerated below.

Table I
Furnace data

Nominal Capacity	150 kg
Power	90 kW
Frequency	2200 Hz
Inner Diameter	0,28 m
Depth	0,56 m

Microwave instrumentation

- Vector Network Analyser (VNA) type 360B, No. 226003
- Test set frequency converter type 3630A, No. 383002
- Signal generator type 6769B, No. 33001
- Broadband horn antenna 2–18 GHz
- Coaxial cables
- Personal computer

The slag was melted on top of a low carbon steel melt in an induction furnace, with a nominal melting capacity of 150 kg, see Figure 5. For furnace data see Table I. A descriptive picture of the experimental set-up is presented in Figure 6. In the figure it can be seen that some geometrical constraints apply to the experimental set-up as the opening angle of the antenna are large and the diameter of the furnace is relatively small. This means that the antenna must be positioned close to the furnace opening to ensure measurements free from interference from reflecting signals but not too close because of interference from the reactive near field.

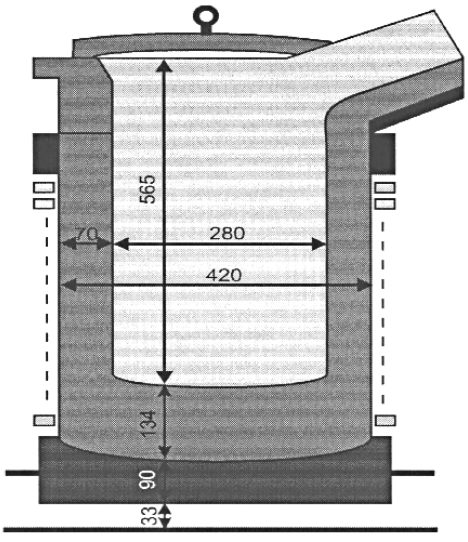

Figure 5. Induction furnace (dimensions in mm)

Table II
Initial synthetic slag mixtures

Slag	Mole fraction			Weight percent			Amount in kg		
No.	xAl_2O_3	xCaO	$xSiO_2$	$\%Al_2O_3$	%CaO	$\%SiO_2$	kg Al_2O_3	kg CaO	kg SiO_2
2	0.00	0.55	0.45	0.00	53.29	46.71	0.00	2.66	2.34
3	0.25	0.75	0.00	37.74	62.26	0.00	1.89	3.11	0.00
4	0.45	0.55	0.00	59.80	40.20	0.00	2.99	2.01	0.00
6	0.20	0.35	0.45	30.41	29.27	40.32	1.52	1.46	2.02
7	0.35	0.35	0.30	48.66	26.76	24.58	2.43	1.34	1.23
8	0.15	0.55	0.30	23.84	48.07	28.09	1.19	2.40	1.40

Trial performance

The measurements were performed in the furnace, and the steel melt served as reference position during the trials. In Figure 6 is a photograph showing the experimental set-up with the antenna positioned directly above the furnace. To avoid oxidation of the sample by the ambient air, the furnace was covered by a ceramic lid and the furnace volume under it was flushed with Argon gas during the measurements. The lid that is made of Slip Cast and Sintered Fused Silica is transparent to microwaves and opaque to heat radiation. It also serves as a protection for the antenna and cables against heat radiation from the furnace.

Before charging the slag sample, aluminium was added to the steel melt to ensure a low oxygen potential in the melt and a minimum of reoxidation reactions between steel and slag during the experiments. The melting of the slag required between 30 and 60 minutes, depending on the slag quality. When the slag sample was totally melted, the microwave measurements started. Slag samples were extracted at the beginning and at the end of the microwave measurements.

Slag mixtures

The slag used was premixed to cope with the requirement of a 5 cm thick liquid slag. With this approach, the experimental set-up is optimized for signal processing. In Table II the initial slag mixtures before melting are presented.

Results

The melting was performed using normal refractor lining material. This affected the initial slag composition as seen in Table III where results from the slag samples during melting are presented. In the table samples L406-1 to L411-1 were taken at the start of measurements and samples L406-2 to L411-2 at the end of measurements.

The results of the refractive index observed for the different slags at different frequency bands are presented in Table IV. The slag temperature during the series of trials varied between 1550 and 1600ºC. Figure 8 shows the measured refractive indexes for the frequency regions 2–6 GHz, 4–8 GHz and 6–10 GHz.

Discussion

Originally the series of trials was planned to comprise slag from the Al_2O_3-CaO-SiO_2 system in quantities presented in Table II. In order to avoid contamination of the synthetic slag due to refractory wear, the original approach was to use a graphite crucible of sufficient volume. However, due to geometrical constraints, requiring a furnace opening with a furnace diameter larger than 0.25 m, and a crucible wall thickness of 0.03 m a standard crucible of that size could not be found or manufactured and standard refractory, acid and basic, therefore had to be used. Using a graphite crucible with an opening less than 0.25 m would have interfered with the antenna beam, resulting in a poor signal performance during the measurements. Therefore the

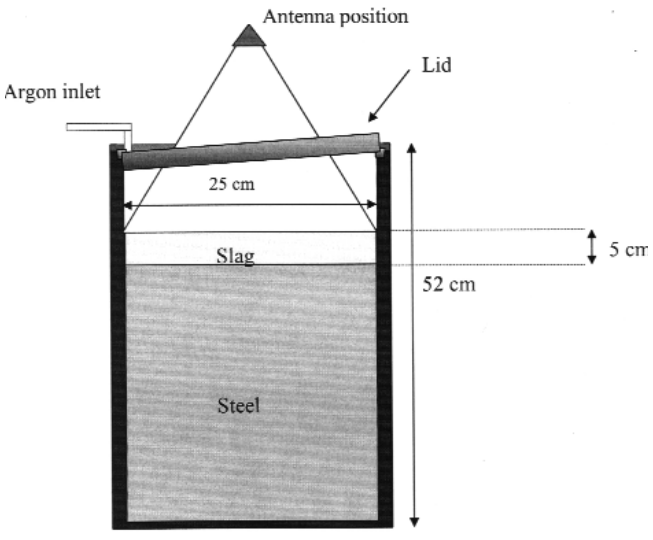

Figure 6. Experimental set-up, schematic

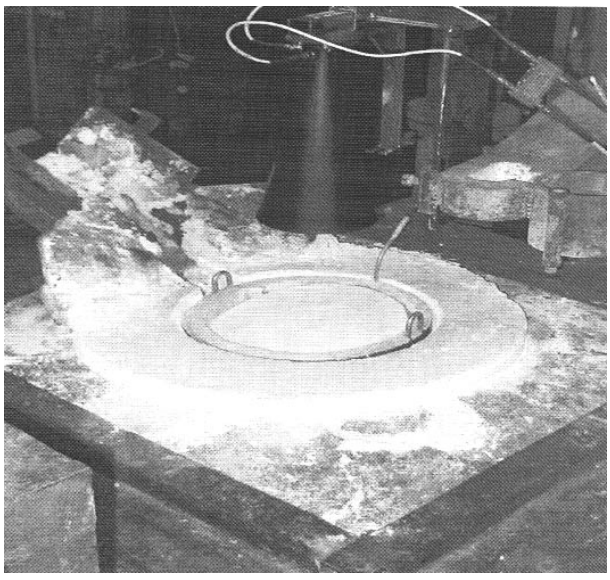

Figure 7. Antenna position during measurement

Table III
Chemical analysis of investigated liquid slags

Charge protocol		Slag analysis wt %					
Sample No.	**Slag type**	**Al_2O_3**	**CaO**	**FeO**	**MgO**	**MnO**	**SiO_2**
L.406-1	Synthetic slag 2	18.49	35.31	3.00	0.40	1.30	40.09
L.406-2		32.66	24.42	2.78	0.37	1.34	36.63
L.407-1	Synthetic slag 7	47.36	19.59	2.73	0.18	1.41	27.84
L.407-2		48.26	18.90	2.64	0.16	1.73	27.68
L.408-1	Synthetic slag 6	35.53	21.67	2.12	0.19	1.81	38.00
L.408-2		36.57	20.02	3.15	0.16	2.20	36.57
L.409-1	Synthetic slag 4	56.70	29.00	1.43	0.30	0.78	10.79
L.409-2		58.80	26.22	1.26	0.22	0.75	11.71
L.410-1	Synthetic slag 8	20.89	35.13	1.79	6.94	1.74	32.88
L.410-2		20.90	34.35	1.27	9.73	1.43	31.57
L.411-1	Synthetic slag 3	30.78	46.81	0.60	11.27	0.17	9.82
L.411-2		29.50	44.07	0.86	14.93	0.33	9.93

results obtained must not be confused with the original slag mixtures since it is obvious that the measurements have been performed on new slag compositions due to contamination of the original slag by refractory ware.

By measuring the refractive index of a slag, a picture of the dielectric properties of that slag may be found. Thus, as the dielectric constant ϵ indirectly reflects the movement of molecules in matter, and the structure of slag is strongly dependent on the composition, the actual slag composition may be ascertained by the refractive index of the slag.

Detailed information about the structures of oxide melts has been derived from X-ray diffraction studies[4]. Based on the results of these studies and the information on viscosities and electric conductivities, the different oxides may be divided into ionic and covalent bond oxides. Metal oxides are generally ionic in nature. This is indicated by the low viscosities and high electrical conductivities in the liquid phase. The conductivities of metal oxides are usually much higher than those of the ionic halides. The high conduction arises either from normal semi-conduction or the jump of localized electrons between ions of varying charge, e.g. Fe^{2+} and Fe^{3+}.

Of special importance are the covalent oxides, in which the oxygen is bound to form three-dimensional networks such as SiO_2, P_2O_5 and AL_2O_3. These oxides give rise to highly viscous melts with very low electrical conductivities. The low conductivities confirm that the bonding is covalent and the high viscosities indicate that the three-dimensional network of the crystals is retained on fusion.

In Figure 9 the refractive index is plotted against the slag basicity in order to show the composition dependency of the refractive index. In the figure the basicity is defined as the ratio $(CaO+MgO)/(Al_2O_3+SiO_2)$. A trend of an increasing refractive index with an increasing basicity may be observed. Generally the refractive index of a polar matter should exhibit a higher value than a non-polar matter. The observed increase of the refractive index with increasing slag basicity is in line with this as a higher basicity would give a break-up of the covalent bondings between silica tetrahedras and therefore give a more polar matter.

As can be seen from Table IV the success rate is approximately 31% (probable and accepted) and thus the significance of the measurements is too low to be

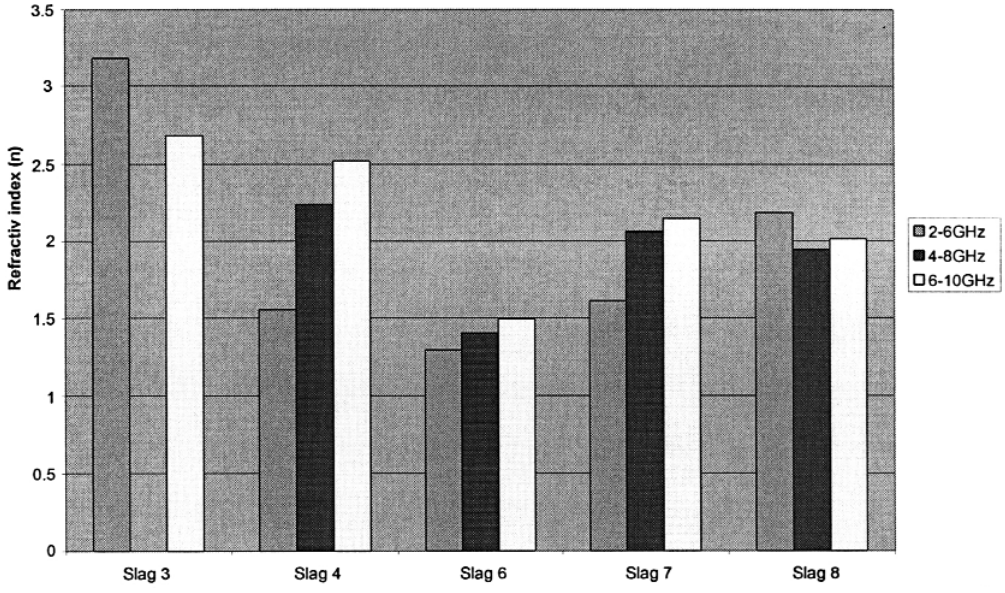

Figure 8. Measured refractive indexes for the frequency regions 2–6 GHz, 4–8 GHz and 6–10 GHz

Table IV
Refractive index observed for the different liquid slags at different frequency regions

Slag quality	Frequency step(GHz)						
	2–6	4–8	6–10	8–12	10–14	12–16	14–18
Synthetic slag 2	-	-	-	-	-	-	-
Synthetic slag 7	1.613	2.064	2.147	1.738	2.247**	1.810**	1.810**
Synthetic slag 6	1.295	1.406	1.496	-	2.039**	2.414**	2.129**
Synthetic slag 4	1.556	2.238*	2.521**	-	1.882*	-	-
Synthetic slag 8	2.185**	1.945	2.017	2.821**	-	-	3.875**
Synthetic slag 3	3.179*	-	2.683*	3.724*	4.200*	-	-
Accepted S/N>7, *Probable 3<S/N<7, **Ambiguous S/N<3							

conclusive. The low success rate can, to some extent, be explained by the experimental set-up but also by the fact that some of the slag qualities were difficult to measure. Another interesting observation is that the success rate declines with increasing frequency and that no values of the refractive index are recorded within the 14–18 GHz frequency band. Most of the approved data emanates from the lower frequency bands 2–6 GHz and 4–8 GHz.

Conclusions

The experiments show that the technology has the potential to become an important tool for on-line process control. However, there is still work to be performed before this can be accomplished, especially due to the composition of slag.

Future work

A new series of trials are planned and a graphite crucible with sufficient dimensions is under production.

References

1. NYFORS, E. and VAINIKAINEN, P., INDUSTRIAL MICROWAVE SENSORS: Ebbe Nyfors & Pertti Vainikainen , Artech House, ISBN 0-89006-397-4
2. Electromagnetic Horn antennas: A.W. Love, IEEE Press NY 1997
3. Antenna Theory: Analysis and design. Constantine A. Balanis, ISBN 0-471-60639-1
4. F. D. RICHARDSON, Physical Chemistry of Melts in Metallurgy, vol. 1, Academic Press London, 1974.

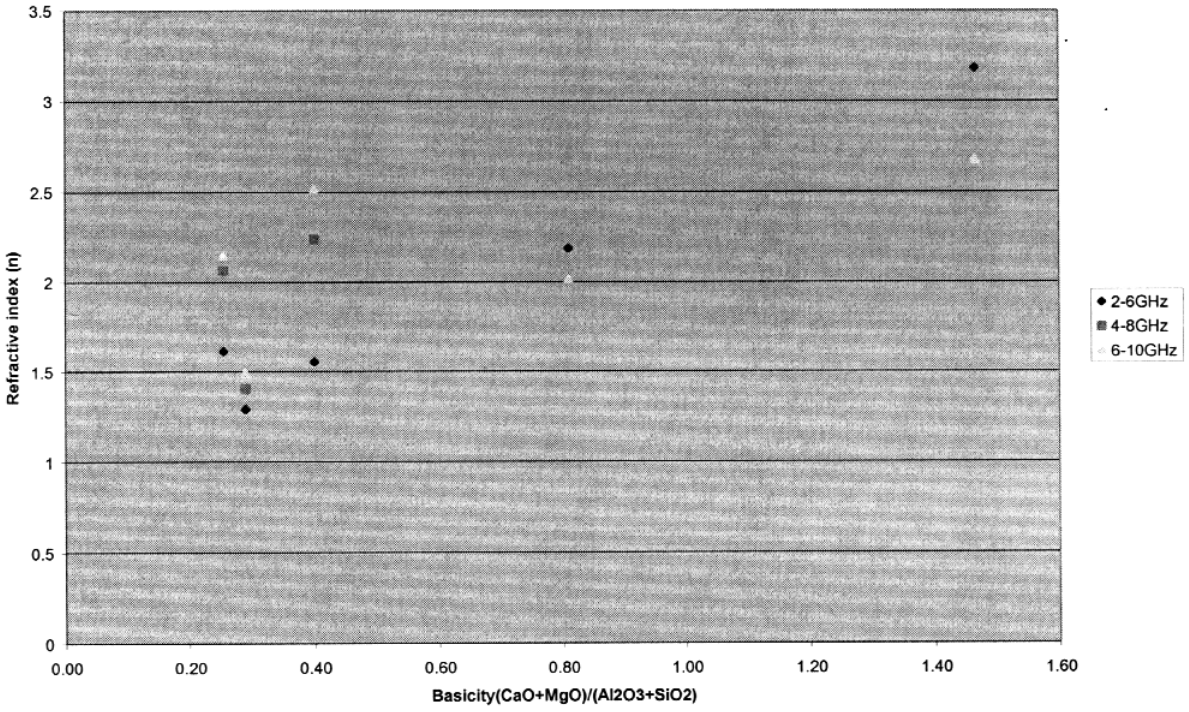

Figure 9. The refractive index as a function of the slag basicity defined as $(CaO+MgO)/(Al_2O_3+SiO_2)$